

TECHNICAL ADVANCE

Open Access



# A standardized approach for exact CT-based three-dimensional position analysis in the distal tibiofibular joint

Firas Souleiman<sup>1\*†</sup>, Martin Heilemann<sup>2†</sup>, Robert Hennings<sup>1</sup>, Mareike Hennings<sup>1</sup>, Alexis Klengel<sup>3</sup>, Pierre Hepp<sup>1</sup>, Georg Osterhoff<sup>1</sup> and Annette B. Ahrberg<sup>1</sup>

## Abstract

**Background:** Assessment of tibiofibular reduction presents an intra- and postoperative challenge. Numerous two-dimensional measurement methods have been described, most of them highly dependent on leg orientation and rater. Aim of the present work was to develop a standardized and orientation-independent 3D based method for the assessment of syndesmotic joint position.

**Methods:** In a retrospective single center study, 3D models of bilateral ankle joints, either after unilateral syndesmosis stabilization (operative group) or with no injury (native group) were superimposed (best fit matching) and aligned uniformly. Based on center of gravity calculations three orientation- and rater-independent parameters were determined: tibiofibular clears space (CS), vertical offset between both fibulae, and translation angle of the fibulae about tibia axis.

**Results:** Bilateral CT datasets of 57 native and 47 postoperative patients were analyzed. In the native group mean CS was 2.7 (SD, 0.8; range, 0.7–4.9) mm, mean CS side difference was 0.62 (SD, 0.45) mm and mean translation angle was 1.6 (SD, 1.4) degrees regarding absolute values. The operative group was found to show a significantly higher CS side difference of 0.88 (SD, 0.75) mm compared to native group ( $P = .046$ ). Compared to the healthy contralateral side, operated fibulae showed mean proximal displacement of 0.56 (SD, 1.67) mm ( $P = .025$ ), dorsal displacement of 1.5 (SD 4.1) degrees ( $P = .017$ ).

**Conclusion:** By using 3D best fit matching, orientation- and rater-dependent errors can be minimized. Large inter-individual and small intraindividual differences of uninjured couples support previous recommendations for bilateral imaging.

*Trial registration:* AZ 131/18-ek; AZ 361/19-ek

**Level of evidence:** Level III.

**Keyword:** Syndesmosis, 3D Position control, Tibiofibular, Ankle, Clear space, CT

## Background

Frequently, ankle fractures are associated with an injury to the distal syndesmosis in up to 45% of the cases [1–4]. Correct reduction of the fibula into the fibular notch of the tibia is a key factor for positive long-term outcome and a major evidence-based criterion of prognostic relevance in ankle fractures [5–11]. A lateral displacement

\*Correspondence: [frs.souleiman@medizin.uni-leipzig.de](mailto:frs.souleiman@medizin.uni-leipzig.de)

<sup>†</sup>Firas Souleiman and Martin Heilemann contributed equally to this work.

<sup>1</sup> Department of Orthopaedics, Trauma and Plastic Surgery, University Hospital Leipzig, Leipzig, Germany

Full list of author information is available at the end of the article



of the fibula by 1 mm already reduces the contact area between talus and tibia by up to 40% [12–15]. Conventional radiography is unreliable to rule out malpositioning of the fibula. Post- or intraoperative bilateral computed tomography (CT) is the most sensitive and specific method to detect malreduction of the tibio-fibular joint [8–10, 16–26]. Even with CT, several different measurements are required to optimally assess the syndesmosis position [10, 22, 27–40]. Schon et al. described three measurements for rotation, lateral and anterior-posterior orientation of the fibula as most specific CT measurements of ankle syndesmotric malreduction [41]. The results of their study presented surprisingly low native side-to-side correlation across all 35 tested measurement methods. Overall, the methods varied considerably in their ability to detect malreduction and an accurate reduction. Proper positioning of the fibula is essential in order to restore the anatomic relationships [42].

Since three-dimensional (3D) assessment has become increasingly important in surgery in recent years, the aim of this study was to establish a standardized 3D based measurement technique for evaluation of the syndesmosis and to provide reference values for this procedure. Furthermore, this methodology should be independent on leg orientation differences and rater independent regarding landmark detection. The major hypothesis of this study was that side differences were significantly higher in unilateral surgically treated ankles compared to native ankles in terms of 3D parameters developed. Secondary, necessity of bilateral CT for exact position control of the syndesmosis should be assessed.

## Methods

The study protocol has been approved by the local institutional review board (Ethical Committee at the Medical Faculty, Leipzig University, AZ 131/18-ek; AZ 361/19-ek). In a retrospective single center (Level I Trauma Center) study, 47 consecutive bilateral CT examinations of patients with a unilateral syndesmotric injury (operative group) in the period from 2008 to 2017 and 57 bilateral CT examinations of uninjured ankle joints (native group) in the period from 2010 to 2019 were included.

Demographic data of interest were age, gender and injured side. In the operative group, all CT examinations were performed after ankle fixation with a syndesmotric screw (3.2 mm, DePuy-Synthes, West Chester, PA), or a suture-button device (TightRope<sup>®</sup>, Arthrex, Naples, FL). Inclusion criteria of the operative group were AO 44 B and C fractures with intraoperative pathological hook test and stabilization of the syndesmosis, anatomic fixation of the fracture components, an inconspicuous contralateral side and imaging of at least 10 cm of the distal lower leg as well as the entire talus. Exclusion criteria

were missing postoperative bilateral CT, trauma of the non-operated side in the past, insufficient CT scans that did not include the fixation device.

Scan types for the native group were CT angiographies with intravenous contrast medium of either the lower extremities (n=52) or the whole body including the lower extremities (n=5). Patients in both groups were older than 18 years and had no relevant bony pathology besides the fracture in the operative group.

CT imaging was performed with two different multi-detector CT scanners (operative group: iCT 256; native group: Ingenuity 128; Philips, Best, The Netherlands). Routine scan parameters varied between the scanners and scan types: Tube current of 100 mAs to 226 mAs, tube voltage of 100 kV or 120 kV, collimation of 64 mm × 0.625 mm or 128 mm × 0.625 mm, pitch of 0.400 to 0.759 and a rotation time of 0.750 s to 0.925 s. In-plane resolution was < 1 mm. Slice thickness of axial reformations was 0.67 mm to 2 mm. Only CT examinations that show the bony structures at least 10 cm proximal to the distal tibia plateau were evaluated.

All patients had given informed consent before surgery and CT scan. In the operative group, open reduction and fixation of the ankle fractures was performed through a lateral approach to the fibula with a lag screw and neutralization plate. In case of additive medial malleolar fractures, a standard medial approach with open reduction and screws, plate or both have been performed.

In case of a posterior tibial fragment (Volkman's triangle), nine patients were operatively stabilized by a dorsal plate or indirect by anterior–posterior lag screws. Syndesmotric instability was tested by the hook test under fluoroscopy [43–45]. In case of instability the surgeon chose between a transsyndesmotric screw and a suture-button device (TightRope<sup>®</sup>) by preference. Standard fluoroscopy (lateral and mortise view) was applied intraoperatively to identify the reduction.

## Assessment of the 3D models

After the operative treatment CT data sets of native and operative group were segmented using a 3D image processing software (Mimics 22.0, Materialise, Leuven, Belgium). In case of enclosed implants, these were virtually removed. Resulting holes were filled virtually with respect to the anatomical geometry. Finally, stereolithographic models (STLs) were created and exported for three-dimensional measurement.

## Data transformation and parameter determination

Data transformation and parameter determination were executed by using Geomagic Design X 2016 (3D Systems, Rock Hill, SC). Prior to any parameter determination, a standardized global alignment of the lower leg bones had

to be established. In this context, two planes orthogonal to the scanning axis, the first 50 mm proximal and the second 100 mm proximal to the tibial articular surface of the left leg, were regarded. The centroids of the tibial cross sections within both planes were calculated and the straight line connecting both points defined the left tibia axis, representing the z-axis for each dataset, respectively. This axis definition prevents parameter discrepancies due to different global orientation of different datasets.

Following this, both STLs, tibia and fibula, were merged for both sides. Hence, the relative position of the fibula with respect to the tibia of the same side was fixed. The right side was mirrored and superimposed with the contralateral side by best fit matching. The distal 100 mm of both tibiae served as relevant geometry for

the matching step. An area of this size was used to ensure accurate matching results even in case of extensive tibial injuries. This procedure enabled to visually identify misalignments between both fibulae.

Since the distal syndesmosis was the area of interest, left tibia, left fibula, and right tibia were cut 20 mm proximal to the tibial articular surface of the left leg. With regard to center of volume calculations, to be implemented in the following, the right fibular part had to be as long as the left one. Differences in length between both fibulae would have a considerable effect on center of volume calculations and, thus, disturb actual measurements. Therefore, the length of the left fibula was measured and then the right fibula was cut at same length (Fig. 1). By contrast, the distal tibial parts were

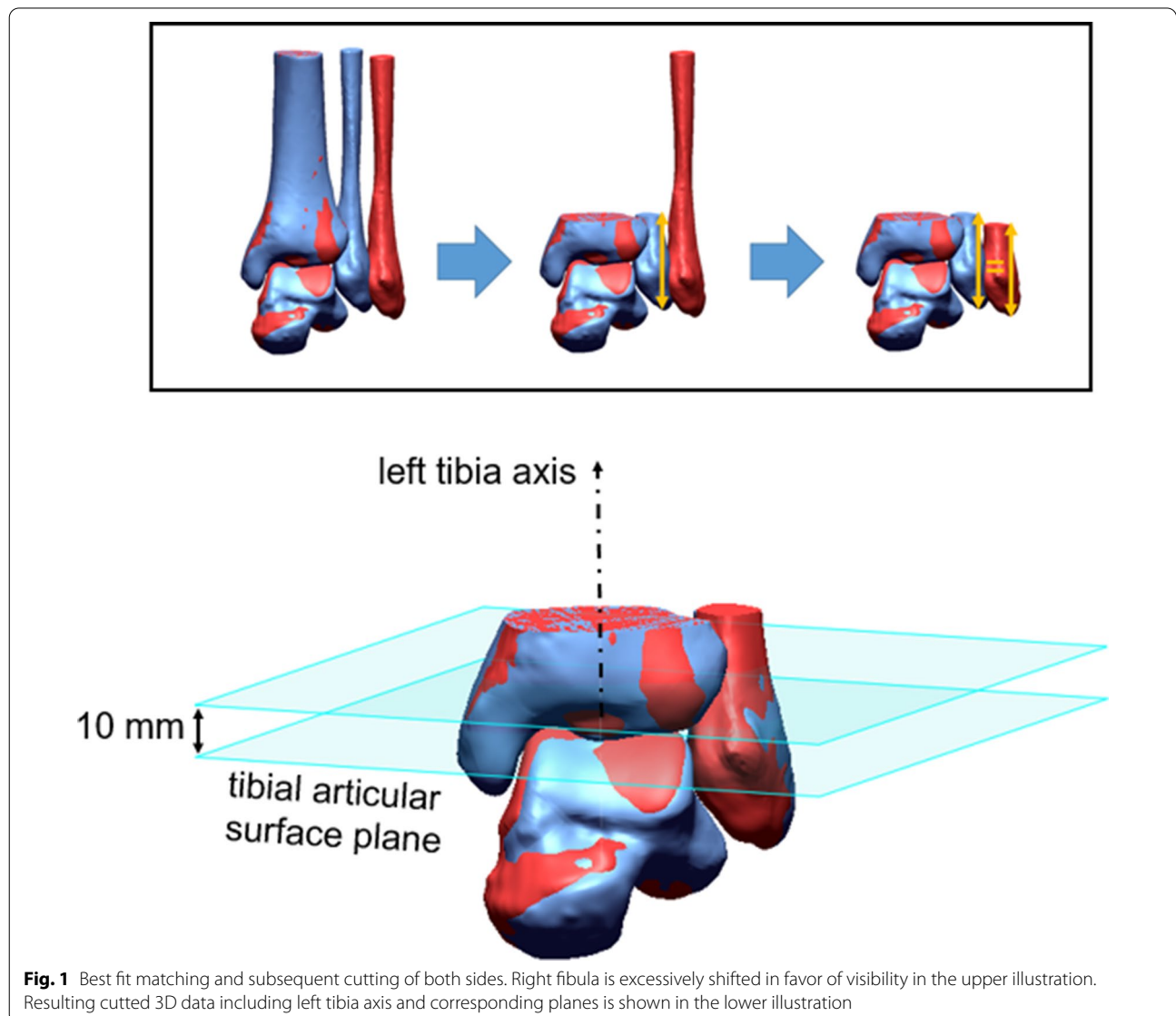


**Fig. 1** Best fit matching and subsequent cutting of both sides. Right fibula is excessively shifted in favor of visibility in the upper illustration. Resulting cutted 3D data including left tibia axis and corresponding planes is shown in the lower illustration

assumed to be equally long, since superimposition of both sides due to best fit matching was performed based on tibial geometry. STLs were transformed to solids by methods of reverse engineering.

Subsequently, centers of volume of tibial and fibular part were calculated for both sides. The left side was set as reference for the native group, the uninjured side for the operative group. Connection vectors of tibial and fibular centers of volume on reference side ( $\vec{r}_0$ ) and contralateral side ( $\vec{r}_1$ ) were used to identify three-dimensional misalignments between both fibulae relative to superimposed tibia alignment. This three-dimensional misalignment was quantified by two parameters: vertical offset ( $\Delta z$ ) along previously defined left tibia axis and translation angle ( $\Delta\alpha$ ) about this axis (Fig. 2).

Since left tibia axis represents the z-axis of the coordinate system, fibular offset is equal to the z-component of the difference vector of both center of volume connections:

$$\Delta z = r_1^{(z)} - r_0^{(z)}$$

Positive differences imply proximal offset with respect to the reference fibula, negative differences imply distal offset.

Fibular rotation about tibia axis is defined as the angle between the projection of both connection vectors into a perpendicular plane, for example the plane defined by  $z = 0$ , and can be calculated via cross product of both vectors:

$$\Delta\alpha = \arcsin\left(\frac{r_0^{(x)} \cdot r_1^{(y)} - r_0^{(y)} \cdot r_1^{(x)}}{\sqrt{r_0^{(x)2} + r_0^{(y)2}} \cdot \sqrt{r_1^{(x)2} + r_1^{(y)2}}}\right)$$

Positive angles imply external rotation about tibia axis, negative angles imply internal rotation.

Furthermore, a landmark independent measurement of tibiofibular clear space was implemented. Clear space was regarded within the plane, perpendicular to left tibia axis, 10 mm proximal to the tibial articular surface of the left leg. Tibial and fibular centroids within this plane were calculated. The straight line through tibial and fibular centroids for both sides intersect tibial and fibular bone contour. Distance between these two intersections defines the clear space in our study (Fig. 3). Tibiofibular clear space difference ( $\Delta CS$ ) is defined as difference between reference side ( $CS_0$ ) and opposite side ( $CS_1$ ):

$$\Delta CS = CS_1 - CS_0$$

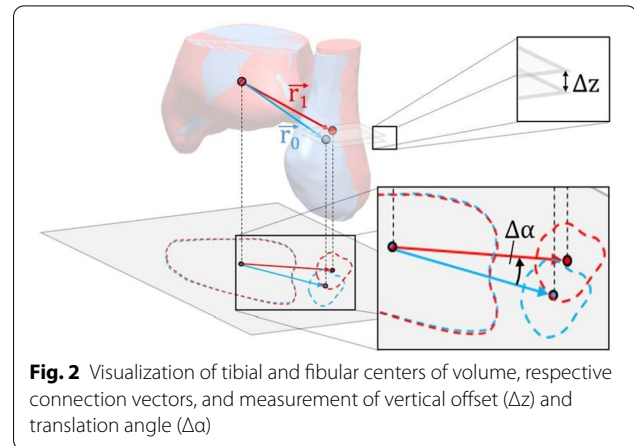


**Fig. 2** Visualization of tibial and fibular centers of volume, respective connection vectors, and measurement of vertical offset ( $\Delta z$ ) and translation angle ( $\Delta\alpha$ )

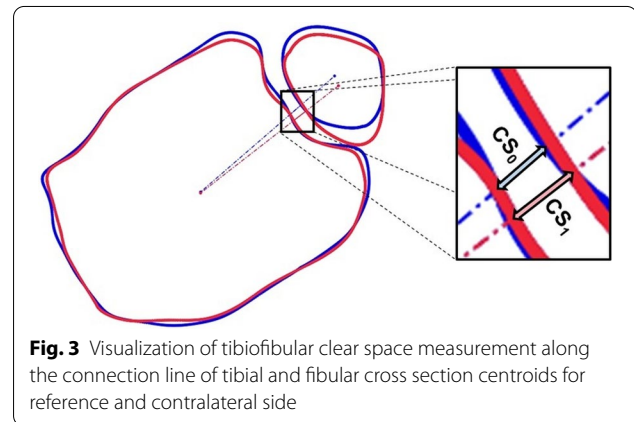


**Fig. 3** Visualization of tibiofibular clear space measurement along the connection line of tibial and fibular cross section centroids for reference and contralateral side

### Statistical analysis

Statistical data analysis was performed by using Matlab (Mathworks, Natick, MA) and G\*Power (HHU Düsseldorf, Germany). Absolute values of all parameters were compared regarding native and operative group. Wilcoxon rank-sum tests (one-tailed) were used to check statistical significance of group-specific differences. Furthermore, operative parameters were compared to 0 mm or  $0^\circ$ , respectively, in order to identify some systematical operative misalignments: oversized / undersized clear space, proximal / distal vertical offset, external / internal translation angle. Those directions were indicated by the sign of the parameters. One-sample *t* tests (two-tailed) were used to check statistical significance of those directions. Level of significance was set at  $P < 0.05$  for both test types.

### Results

Demographic data of the native and operative patient groups are shown in Table 1. Age and gender distribution of both groups were comparable. According to the

**Table 1** Demographic data of all patients

Group	Number	Gender		Age in years		
		Male	Female	Mean	SD	Min   Max
native	57	39	18	53	18	18   90
operative	47	30	17	48	18	24   87
<i>P</i> value		.68			.19	

AO classification, there were 19 AO 44 B and 28 AO 44 C fractures in the operative group [46].

The 114 legs of the native group showed a mean tibiofibular clear space of 2.7 (SD, 0.8) mm. Measured native clear spaces ranged from 0.7 mm to 4.9 mm. All 47 operatively treated legs showed a mean tibiofibular clear space of 3.5 (SD, 1.7; range, 0.1–9.1) mm, whereas contralateral uninjured leg showed a mean clear space of 3.2 (SD, 1.0; range, 1.6–5.8) mm.

In order to evaluate tibiofibular reduction, clear space differences between both legs were analyzed. The median tibiofibular clear space difference, regarding absolute values, was 0.55 mm for the native group and 0.68 mm for the operative group.

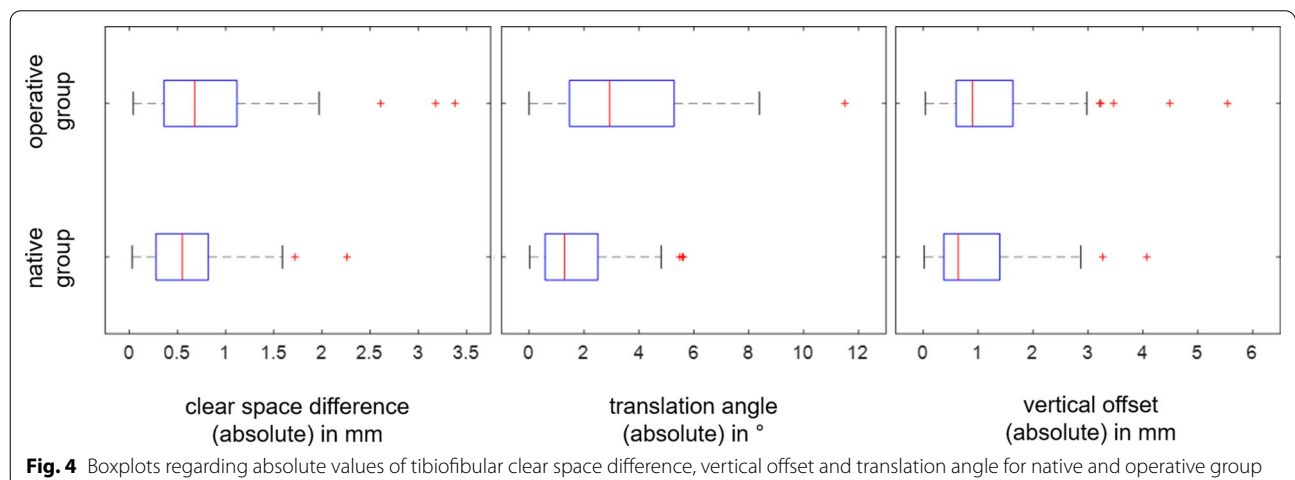
Furthermore, vertical offset and translation angle with respect to the reference side were used to identify misalignments. Boxplots in Fig. 4 show absolute values of clear space difference, vertical offset and translation angle for native and operative group, respectively. In the operative group, a clear space difference exceeding 2 mm was found in 3 of 47 patients (6.3%), a vertical offset exceeding 3 mm in 5 patients (10.6%), and a translation angle exceeding 5 degrees in 12 patients (25.5%). In the native group, a clear space difference exceeding 2 mm was found in 1 of 57 patients (1.7%), a vertical offset exceeding 3 mm in 2 patients (3.5%), and a translation angle exceeding 5 degrees in 3 patients (5.2%).

Figure 5 shows histograms for all three parameters with consideration of their sign. This allows identification of systematic misalignment direction of operative group in comparison to the native group.

Hypothesis tests and decisions are shown in Table 2. According to those tests, absolute tibiofibular clear space difference, vertical offset, and translation angle of operative group are significantly larger compared to native group. Furthermore, directions of misalignment after surgery regarding vertical offset and translation angle were identified. Mean vertical offset is +0.56 (SD, 1.67) mm and significantly different from zero which indicates proximal offset. Mean translation angle is +1.5 (SD, 4.1) degrees and also significantly different from zero which indicates external rotation. Mean tibiofibular clear space difference after surgery is +0.23 (SD, 1.14) mm, but with the numbers available, no significant direction of misalignment could be detected. A post-hoc power analysis showed a power of 0.27 for this hypothesis test.

**Discussion**

The main objective of the work, the development of a three-dimensional measurement method for the exact assessment of the syndesmosis position in order to eliminate limitations of the previously used methods, was achieved. Since all three developed parameters showed significantly larger side differences in the operative group



**Fig. 4** Boxplots regarding absolute values of tibiofibular clear space difference, vertical offset and translation angle for native and operative group

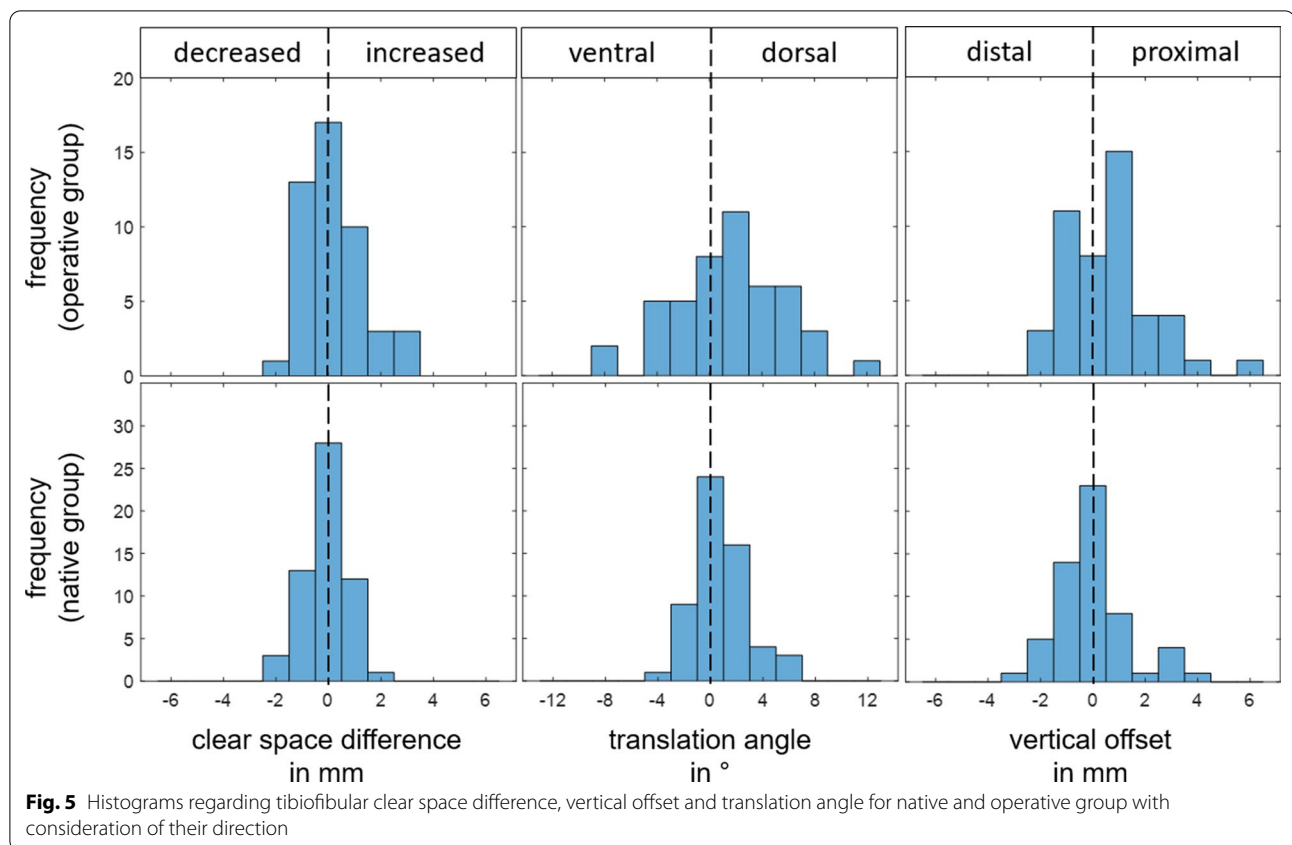


**Table 2** Hypothesis tests ( $\Delta CS$ : tibiofibular clear space difference,  $\Delta z$ : vertical offset,  $\Delta \alpha$ : translation angle, n: native group, o: operative group)

$H_0$	$H_1$	Test	P value	decision
$ \Delta CS_o  =  \Delta CS_n $	$ \Delta CS_o  >  \Delta CS_n $	Wilcoxon rank-sum test	.046	$H_0$ rejected
$ \Delta z_o  =  \Delta z_n $	$ \Delta z_o  >  \Delta z_n $	Wilcoxon rank-sum test	.029	$H_0$ rejected
$ \Delta \alpha_o  =  \Delta \alpha_n $	$ \Delta \alpha_o  >  \Delta \alpha_n $	Wilcoxon rank-sum test	<.001	$H_0$ rejected
$\Delta CS_o = 0$	$\Delta CS_o \neq 0$	One-sample t test	.167	$H_0$ accepted
$\Delta z_o = 0$	$\Delta z_o \neq 0$	One-sample t test	.025	$H_0$ rejected
$\Delta \alpha_o = 0$	$\Delta \alpha_o \neq 0$	One-sample t test	.017	$H_0$ rejected

compared to the native group, the major hypothesis of this study was confirmed.

Slightly different orientation of both legs of a patient is an issue in two-dimensional imaging processes, and thus resulting image planes are tilted against each other. This results in an error in 2D parameter calculations such as clear space measurement [47]. In the present study, these

intra-individual differences in leg orientation were compensated by using three-dimensional datasets, mirroring one side and subsequent best fit matching of both legs. Subsequent considerations of particular planes do not include the tilting error described above.

In addition, three-dimensional data enable a more comprehensive characterization of differences in position compared to two-dimensional data.

Still, interindividual differences in orientation remained an issue. Therefore, one reference tibia axis was determined for each dataset using centroid calculation of tibial cross sections in two clearly defined planes orthogonal to the scanning axis. Although these two planes are subject to potentially slight leg orientation differences, the calculation of the tibial cross-sectional centroids in these planes is almost uninfluenced due to the uniform geometry of the tibia in those regions. Even in a slightly tilted cross-sectional plane, the center of gravity remains centrally located within the tibial geometry. Hence, this procedure enabled consistent axial alignment of each dataset on the basis of respective tibia geometries. Thus, substantially increased interindividual comparability was achieved.

In previous measurement methods anatomical landmarks were selected by an examiner, which resulted

in rater dependent measurement differences [10, 22, 27–40]. In contrast, the methods described in this study avoid rater dependent landmark detection. Instead, centers of volume and area were calculated based on respective three-dimensional geometries and two-dimensional cross sections. Centers of volume were used to calculate the rater independent parameters vertical offset and translation angle. An additional substantial advantage of the centers of volume assessment is its stability to local artifacts of the geometry in contrast to landmark based measurements. Centroids of tibial cross sections enabled rater independent measurement of tibiofibular clear space. Clear space, after three-dimensional adaptation, was used as one of the most frequently used parameters to describe tibiofibular reduction. In order to also describe the remaining two dimensions, the parameters vertical offset and translation angle were introduced. In consequence, displacement in all three dimensions were described.

The translation angle is mainly determined by displacement of the fibula in ventral or dorsal direction. This angle is actually also influenced by possible medialization / lateralization. However, for small angles such as those in the study, this influence is negligible. In addition, medial / lateral displacement is quantified using the clear space differences. Height displacements of both fibulae are exactly described by the vertical offset.

Applying 3D based measurements on unilaterally stabilized ankle joints, a noticeably wider distribution was found compared to the native group. In addition, hypothesis tests confirmed significantly increased absolute values of all three parameters for the operative group. Moreover, absolute results for the native group indicated thresholds for all three parameters according to usual outlier definition using 150% of the interquartile range plus the third quartile. Rounded to the nearest integer, following thresholds resulted: 2 mm for clear space difference, 3 mm for vertical offset and 5 degrees for the translation angle. This is comparable to other clinical and biomechanical studies, where side differences larger than 2 mm are considered relevant [12, 26, 28, 48, 49].

For the operative group, 20 exceedances of those parameter threshold values were detected.

Consideration of the sign of the measured parameters additionally allowed identification of direction of misalignments compared to reference side. According to this study the fibula of the treated leg was significantly proximally shifted and dorsally inclined about tibia axis. This observed systematic direction of malalignment should be considered during intraoperative reduction. Whether this influences the outcome of the surgery remains to be investigated. With regard to differences in tibiofibular clear space, no general direction

was determined for treated legs. However, the test power for this hypothesis was fairly low (0.27) due to the small effect size.

There is also a controversial discussion about the necessity of bilateral CT control after syndesmosis stabilization [9, 10, 21, 24, 26, 28]. Regarding clear spaces measured in this study, the native group exhibited a standard deviation of 0.84 mm whereas the median clear space difference between both sides was 0.55 mm. This indicates a substantially larger interindividual clear space variation compared to intraindividual variation, and thus supports the recommendation from the literature for bilateral imaging.

The authors acknowledge some limitations to the design of the study. The presence of implants that were virtually removed and injured bone structure may affect the accuracy of the CT measurements. CT angiographies were used for the native group, since numerous bilaterally uninjured data sets were available. However, the measurement error resulting from scanning parameter variations was acceptably low in both groups [50]. Furthermore, the consideration of intraindividual side differences also ensures that the calculated parameters are barely influenced by the respective scan type. Other assessment methods including plain radiography, weight-bearing CT/MRI and dynamic testing were not evaluated in this study. It is conceivable that the effects on the measurement parameters in weight-bearing CT/MRI could be greater.

No outcome scores were collected during the study. Thus, no clinical symptoms of complaints can be deduced from the measurement results.

In summary, established measuring methods [41] for assessing syndesmosis can be transferred to a three-dimensional measurement. By using 3D models, best fit matching and center of volume/centroids calculations, leg orientation dependent errors and rater dependent errors can be minimized while all aspects of syndesmosis malreduction will be described sufficient. This is a crucial advantage over two-dimensional measuring methods [42]. Hence, the presented methodology provides diverse potential in future use cases. It can be applied as a diagnostic tool to determine preoperative and postoperative displacement of injured ankle that may be suitable for surgery. It can be used for preoperative planning of correction. The described three-dimensional measurement method, automated on intraoperative 3D imaging, could also be used in the future as a tool for accurate position analysis in real time, thus reducing the number of revision surgeries and providing additional safety to the surgeon. Further measurements are necessary to create a comprehensive three-dimensional database.

**Acknowledgements**

Not applicable.

**Authors' contributions**

Concept and design of the work: Souleiman, Heilemann, R Hennings, Osterhoff, Ahrberg. Preparation and submission of the ethics proposal: Souleiman, M Hennings, Hepp, Osterhoff. Development of a sophisticated measurement methodology for three-dimensional, orientation-independent and rater-independent evaluation: Souleiman, Heilemann. Acquisition of CT data sets (native und operated): Souleiman, R Hennings, M Hennings, Klengel. Segmentation of the CT data sets to create 3D models: Souleiman, R Hennings, M Hennings. Application of the developed measurement methodology to the 3D data sets: Heilemann. Assessment and discussion of the methodology and results: Souleiman, Heilemann, R Hennings, Hepp, Osterhoff, Ahrberg. Drafting the manuscript: Souleiman, Heilemann. Reviewing the manuscript: M Hennings, R Hennings, Klengel, Hepp, Osterhoff, Ahrberg. All authors read and approved the final manuscript.

**Funding**

Open Access funding enabled and organized by Projekt DEAL. The authors received no financial support for the research, authorship, and/or publication of this article.

**Availability of data and materials**

The datasets used and/or analyzed during the current study are available from the corresponding author on reasonable request.

**Declarations****Ethics approval and consent to participate**

The study protocol has been approved by the local institutional review board (Ethical Committee at the Medical Faculty, Leipzig University, AZ 131/18-ek; AZ 361/19-ek). The authors declare that the study was performed in accordance with the ethical standards as laid down in the 1964 Declaration of Helsinki and its later amendments or comparable ethical standards.

**Consent for publication**

Informed consent was obtained from all patients.

**Competing interests**

The authors declare no conflict of interest with respect to the research, authorship, and/or publication of this article.

**Author details**

<sup>1</sup> Department of Orthopaedics, Trauma and Plastic Surgery, University Hospital Leipzig, Leipzig, Germany. <sup>2</sup> ZESBO - Centre for Research On Musculoskeletal Systems, University of Leipzig, Leipzig, Germany. <sup>3</sup> Department of Radiology, University Hospital Leipzig, Leipzig, Germany.

Received: 27 October 2020 Accepted: 18 February 2021

Published online: 06 March 2021

**References**

- Purvis GD. Displaced, unstable ankle fractures: classification, incidence, and management of a consecutive series. *Clinical orthopaedics and related research*. 1982;:91–8.
- Jensen SL, Andresen BK, Mencke S, Nielsen PT. Epidemiology of ankle fractures: a prospective population-based study of 212 cases in Aalborg, Denmark *Acta Orthopaedica Scandinavica*. 1998;69:48–50.
- Zalavras C, Thordarson D. Ankle syndesmotic injury. *JAAOS*. 2007;15:330–9.
- Tornetta P III, Axelrad TW, Sibai TA, Creevy WR. Treatment of the stress positive ligamentous SE4 ankle fracture: incidence of syndesmotic injury and clinical decision making. *J Orthop Trauma*. 2012;26:659–61.
- Chissell HR, Jones J. The influence of a diastasis screw on the outcome of Weber type-C ankle fractures. *J Bone Joint Surg Br Vol*. 1995;77:435–8.
- Mont MA, Sedlin ED, Weiner LS, Miller AR. Postoperative radiographs as predictors of clinical outcome in unstable ankle fractures. *J Orthop Trauma*. 1992;6:352–7.
- Naqvi GA, Shafiqat A, Awan N. Tightrope fixation of ankle syndesmosis injuries: clinical outcome, complications and technique modification. *Injury*. 2012;43:838–42.
- Rammelt S, Zwipp H, Grass R. Injuries to the distal tibiofibular syndesmosis: an evidence-based approach to acute and chronic lesions. *Foot Ankle Clin*. 2008;13:611–33.
- Sagi HC, Shah AR, Sanders RW. The functional consequence of syndesmotic joint malreduction at a minimum 2-year follow-up. *J Orthop Trauma*. 2012;26:439–43.
- Vasarhelyi A, Lubitz J, Gierer P, Gradl G, Rösler K, Hopfenmüller W, et al. Detection of fibular torsional deformities after surgery for ankle fractures with a novel CT method. *Foot Ankle Int*. 2006;27:1115–21.
- Wikerøy AK, Høiness PR, Andreassen GS, Hellund JC, Madsen JE. No difference in functional and radiographic results 8.4 years after quadricortical compared with tricortical syndesmosis fixation in ankle fractures. *Journal of orthopaedic trauma*. 2010;24:17–23.
- Thordarson DB, Motamed S, Hedman T, Ebramzadeh E, Bakshian S. The effect of fibular malreduction on contact pressures in an ankle fracture malunion model. *JBSJ*. 1997;79:1809–15.
- Curtis MJ, Michelson JD, Urquhart MW, Byank RP, Jinnah RH. Tibiotalar contact and fibular malunion in ankle fractures A cadaver study. *Acta Orthop Scand*. 1992;63:326–9.
- Moody M, Koeneman J, Hettlinger E, Karpman R. The effects of fibular and talar displacement on joint contact areas about the ankle. *Orthop Rev*. 1992;21:741–4.
- Hunt KJ, Goeb Y, Behn AW, Criswell B, Chou L. Ankle joint contact loads and displacement with progressive syndesmotic injury. *Foot Ankle Int*. 2015;36:1095–103.
- Magid D, Michelson JD, Ney D, Fishman EK. Adult ankle fractures: comparison of plain films and interactive two-and three-dimensional CT scans. *AJR Am J Roentgenol*. 1990;154:1017–23.
- Ebraheim NA, Lu J, Yang H, Mekhail AO, Yeasting RA. Radiographic and CT evaluation of tibiofibular syndesmotic diastasis: a cadaver study. *Foot Ankle Int*. 1997;18:693–8.
- Harper MC. Delayed reduction and stabilization of the tibiofibular syndesmosis. *Foot Ankle Int*. 2001;22:15–8.
- Beumer A, Van Hemert W, Niesing R, Entius C, Ginai A, Mulder P, et al. Radiographic measurement of the distal tibiofibular syndesmosis has limited use. *Clinical Orthopaedics and Related Research* (1976–2007). 2004;423:227–34.
- Gardner MJ, Demetrakopoulos D, Briggs SM, Helfet DL, Lorch DG. Malreduction of the tibiofibular syndesmosis in ankle fractures. *Foot Ankle Int*. 2006;27:788–92.
- Miller AN, Carroll EA, Parker RJ, Boraiah S, Helfet DL, Lorch DG. Direct visualization for syndesmotic stabilization of ankle fractures. *Foot Ankle Int*. 2009;30:419–26.
- Marmor M, Hansen E, Han HK, Buckley J, Matiyahu A. Limitations of standard fluoroscopy in detecting rotational malreduction of the syndesmosis in an ankle fracture model. *Foot Ankle Int*. 2011;32:616–22.
- Ruan Z, Luo C, Shi Z, Zhang B, Zeng B, Zhang C. Intraoperative reduction of distal tibiofibular joint aided by three-dimensional fluoroscopy. *Technol Health Care*. 2011;19:161–6.
- Song DJ, Lanzi JT, Groth AT, Drake M, Orchowski JR, Shaha SH, et al. The effect of syndesmosis screw removal on the reduction of the distal tibiofibular joint: a prospective radiographic study. *Foot Ankle Int*. 2014;35:543–8.
- Rammelt S, Obruba P. An update on the evaluation and treatment of syndesmotic injuries. *Eur J Trauma Emerg Surg*. 2015;41:601–14.
- Ahrberg AB, Hennings R, von Dercks N, Hepp P, Josten C, Spiegl UJ. Validation of a new method for evaluation of syndesmotic injuries of the ankle. *International orthopaedics*. 2020.
- Ahn T-K, Choi S-M, Kim J-Y, Lee W-C. Isolated syndesmosis diastasis: computed tomography scan assessment with arthroscopic correlation. *Arthroscopy: The Journal of Arthroscopic & Related Surgery*. 2017;33:828–34.
- Davidovitch RI, Weil Y, Karia R, Forman J, Looze C, Liebergall M, et al. Intraoperative syndesmotic reduction: three-dimensional versus standard fluoroscopic imaging. *JBSJ*. 2013;95:1838–43.
- Dikos GD, Heisler J, Choplin RH, Weber TG. Normal tibiofibular relationships at the syndesmosis on axial CT imaging. *J Orthop Trauma*. 2012;26:433–8.

30. Elgafy H, Semaan HB, Blessinger B, Wassef A, Ebraheim NA. Computed tomography of normal distal tibiofibular syndesmosis. *Skeletal Radiol.* 2010;39:559–64.
31. Gifford PB, Lutz M. The tibiofibular line: an anatomical feature to diagnose syndesmosis malposition. *Foot Ankle Int.* 2014;35:1181–6.
32. Lepojärvi S, Niinimäki J, Pakarinen H, Koskela L, Leskelä H-V. Rotational dynamics of the talus in a normal tibiotalar joint as shown by weight-bearing computed tomography. *JBJS.* 2016;98:568–75.
33. Lepojärvi S, Pakarinen H, Savola O, Haapea M, Sequeiros RB, Niinimäki J. Posterior translation of the fibula may indicate malreduction: CT study of normal variation in uninjured ankles. *J Orthop Trauma.* 2014;28:205–9.
34. Malhotra K, Welck M, Cullen N, Singh D, Goldberg AJ. The effects of weight bearing on the distal tibiofibular syndesmosis: a study comparing weight bearing-CT with conventional CT. *Foot Ankle Surg.* 2019;25:511–6.
35. Mendelsohn ES, Hoshino CM, Harris TG, Zinar DM. CT characterizing the anatomy of uninjured ankle syndesmosis. *Orthopedics.* 2014;37:e157–60.
36. Nault M-L, Hébert-Davies J, Laflamme G-Y, Leduc S. CT scan assessment of the syndesmosis: a new reproducible method. *J Orthop Trauma.* 2013;27:638–41.
37. Pelton K, Thordarson DB, Barnwell J. Open versus closed treatment of the fibula in Maisonneuve injuries. *Foot Ankle Int.* 2010;31:604–8.
38. Phisitkul P, Ebinger T, Goetz J, Vaseenon T, Marsh JL. Forceps reduction of the syndesmosis in rotational ankle fractures: a cadaveric study. *JBJS.* 2012;94:2256–61.
39. Prior CP, Widnall JC, Rehman AK, Weller DM, Wood EV. A simplified, validated protocol for measuring fibular reduction on ankle CT. *Foot Ankle Surg.* 2017;23:53–6.
40. Tang CW, Roidis N, Vaishnav S, Patel A, Thordarson DB. Position of the distal fibular fragment in pronation and supination ankle fractures: a CT evaluation. *Foot Ankle Int.* 2003;24:561–6.
41. Schon JM, Brady AW, Krob JJ, Lockard CA, Marchetti DC, Dornan GJ, et al. Defining the three most responsive and specific CT measurements of ankle syndesmosis malreduction. *Knee Surgery, Sports Traumatology, Arthroscopy.* 2019;:1–14.
42. Clanton TO, Williams BT, Backus JD, Dornan GJ, Liechti DJ, Whitlow SR, et al. Biomechanical analysis of the individual ligament contributions to syndesmosis stability. *Foot Ankle Int.* 2017;38:66–75.
43. Mizel MS. Technique tip: a revised method of the Cotton test for intra-operative evaluation of syndesmosis injuries. *Foot Ankle Int.* 2003;24:86–7.
44. Stoffel K, Wysocki D, Baddour E, Nicholls R, Yates P. Comparison of two intraoperative assessment methods for injuries to the ankle syndesmosis: a cadaveric study. *JBJS.* 2009;91:2646–52.
45. van den Bekerom MP. Diagnosing syndesmosis instability in ankle fractures. *World journal of orthopedics.* 2011;2:51.
46. Meinberg EG, Agel J, Roberts CS, Karam MD, Kellam JF. Fracture and Dislocation Classification Compendium-2018. *J Orthop Trauma.* 2018;32(Suppl 1):S1-170.
47. Rammelt S, Grass R, Biewener A, Zwipp H. Anatomie, Biomechanik und Klassifikation der Sprunggelenkfrakturen. *Trauma und Berufskrankheit.* 2004;6:S384–92.
48. Berkes MB, Little MT, Lazaro LE, Pardee NC, Schottel PC, Helfet DL, et al. Articular congruity is associated with short-term clinical outcomes of operatively treated SER IV ankle fractures. *JBJS.* 2013;95:1769–75.
49. Ramsey PL, HAMILTON W. Changes in tibiotalar area of contact caused by lateral talar shift. *JBJS.* 1976;58:356–7.
50. Whymys BJ, Vorperian HK, Gentry LR, Schimek EM, Bersu ET, Chung MK. The effect of computed tomographic scanner parameters and 3-dimensional volume rendering techniques on the accuracy of linear, angular, and volumetric measurements of the mandible. *Oral Surg Oral Med Oral Pathol Oral Radiol.* 2013;115:682–91.

## Publisher's Note

Springer Nature remains neutral with regard to jurisdictional claims in published maps and institutional affiliations.

Ready to submit your research? Choose BMC and benefit from:

- fast, convenient online submission
- thorough peer review by experienced researchers in your field
- rapid publication on acceptance
- support for research data, including large and complex data types
- gold Open Access which fosters wider collaboration and increased citations
- maximum visibility for your research: over 100M website views per year

At BMC, research is always in progress.

Learn more [biomedcentral.com/submissions](https://biomedcentral.com/submissions)

